

Charged pions from Ni on Ni collisions between 1 and 2 AGeV

D. Pelte⁶, M. Eskef⁶, G. Goebels⁶, E. Häfele⁶, N. Herrmann^{4,6},
M. Korolija^{6,11}, H. Merlitz^{4,6}, S. Mohren⁶, M. Trzaska⁶,
J.P. Alard³, V. Amouroux³, A. Andronic¹, Z. Basrak¹¹,
N. Bastid³, I. Belyaev⁷, D. Best⁴, J. Biegansky⁵, A. Buta¹,
R. Čaplar¹¹, N. Cindro¹¹, J.P. Coffin⁹, P. Crochet⁹,
P. Dupieux³, M. Dželalija¹¹, J. Erö², P. Fintz⁹, Z. Fodor²,
A. Genoux-Lubain³, A. Gobbi⁴, G. Guillaume⁹,
K.D. Hildenbrand⁴, B. Hong⁴, F. Jundt⁹, J. Kecskemeti²,
M. Kirejczyk^{4,10}, P. Koncz², Y. Korchagin⁷, R. Kotte⁵,
C. Kuhn⁹, D. Lambrecht³, A. Lebedev⁷, I. Legrand¹,
Y. Leifels⁴, V. Manko⁸, J. Mösner⁵, D. Moisa¹, W. Neubert⁵,
M. Petrovici¹, C. Pinkenburg⁴, P. Pras³, F. Rami⁹,
V. Ramillien³, W. Reisdorf⁴, J.L. Ritman⁴, C. Roy⁹,
D. Schüll⁴, Z. Seres², B. Sikora¹⁰, V. Simion¹,
K. Siwek-Wilczynska¹⁰, V. Smolyankin⁷, U. Sodan⁴,
M.A. Vasiliev⁸, P. Wagner⁹, G.S. Wang⁴, T. Wienold⁴,
D. Wohlfarth⁵, A. Zhilin⁷

The *FOPI* Collaboration

September 14, 2018

¹ Institute for Physics and Nuclear Engineering, Bucharest, Romania

² Central Research Institute for Physics, Budapest, Hungary

³ Laboratoire de Physique Corpusculaire, IN2P3/CNRS, and Université Blaise Pascal, Clermont-Ferrand, France

⁴ Gesellschaft für Schwerionenforschung, Darmstadt, Germany

⁵ Forschungszentrum Rossendorf, Dresden, Germany

⁶ Physikalisches Institut der Universität Heidelberg, Heidelberg, Germany

⁷ Institute for Theoretical and Experimental Physics, Moscow, Russia

⁸ Kurchatov Institute, Moscow, Russia

⁹ Centre de Recherches Nucléaires and Université Louis Pasteur, Strasbourg, France

¹⁰ Institute of Experimental Physics, University of Warsaw, Poland

¹¹ Rudjer Boskovic Institute, Zagreb, Croatia

Abstract

Charged pions from Ni + Ni reactions at 1.05, 1.45 and 1.93 AGeV are measured with the *FOPI* detector. The mean π^\pm multiplicities per mean number of participants increase with beam energy, in accordance with earlier studies of the Ar + KCl and La + La systems. The pion kinetic energy spectra have concave shape and are fitted by the superposition of two Boltzmann distributions with different temperatures. These apparent temperatures depend only weakly on bombarding energy. The pion angular distributions show a forward/backward enhancement at all energies, but not the $\Theta = 90^\circ$ enhancement which was observed in case of the Au + Au system. These features also determine the rapidity distributions which are therefore in disagreement with the hypothesis of one thermal source. The importance of the Coulomb interaction and of the pion rescattering by spectator matter in producing these phenomena is discussed.

1 Introduction

This paper presents data on the π^\pm emission from Ni + Ni reactions at bombarding energies 1.06, 1.45, 1.93 AGeV. The data were obtained with the *FOPI* detector at *GSI* and cover almost 4π . They are considered a supplement and extension of a previous study of the Au + Au reaction at 1.06 AGeV which was also performed with the *FOPI* detector [1]. The purpose of our new study is to systematically investigate the dependence of the pion production on system mass and energy in heavy-ion collisions. The present paper is therefore organized in close similarity to ref.[1].

The pion production rate in heavy-ion collisions increases rapidly with bombarding energy. At 14 AGeV the number of pions measured in central collisions has reached the number of baryons contained in the participant [2]. At energies where the number of mesons is still smaller than the number of baryons, calculations based on the BUU model [3] [4] have shown that the number of pions reaches its final value, which is the one measured, only at very late stages of the reaction. At earlier times pions are partly absorbed by the nucleons with the result that a considerable part of the baryons consists of nucleon resonances, primarily of the $\Delta(1232)$ resonance. For the observed properties of pions the concept of their freeze-out time and the complex evolution of the baryon distribution are important considerations. Pions are emitted during the total time of the reaction and thus their phase space distribution bears the signature of the complete reaction history. The early measurements of the pion energy spectra [5] [6] showed that these are quite different from the corresponding proton spectra. Compared to pure Boltzmann spectra with fixed temperature T the former are, at around 1 AGeV bombarding energy, concave shaped with a mean temperature of about $T = 70$ MeV, whereas the latter are convex shaped with a mean temperature of about $T = 100$ MeV. This difference was first interpreted [6] as due to the

different source sizes at freeze-out time, later it was realized [7] that pions mainly originate from the decay of the $\Delta(1232)$ resonance, and that their spectral shape is strongly influenced by the decay kinematics. Therefore pions are very good indicators for the excitation of such resonances. On the other hand, besides the decay channel $\Delta \rightarrow N + n\pi$, also the competing channel $\Delta + N \rightarrow N + N$ determines the fate of the resonances in nuclear matter. The time evolution of the nuclear matter distribution is, in addition to the decay kinematics, the second decisive factor for the pion phase space distributions.

The question of how these processes change with mass and energy of the colliding nuclei motivated the present investigation. The comparison with other reactions particularly include data from ref.[1] and from the work of Harris et al.[8]. Recently corroborative data from other experiments on pion production, performed by the *TAPS* [9] and *KaoS* [10] collaborations at *GSI* have become available. Besides these published results, the more detailed *GSI* reports [9] [10] and conference proceedings, as e.g. ref. [11], are of particular interest for the present investigation.

The paper is organized as follows: The section 2 gives a short summary of the experimental procedures. This part is shortened to the absolute necessary since a more detailed account of these procedures was published in ref.[1]. The section 3 presents the experimental results, frequently data from the Au + Au reaction are included to illuminate the dependence on system mass. The summary and discussion of the results on pion production obtained so far with the *FOPI* detector are contained in section 4.

2 Experimental procedures

The reaction Ni + Ni was studied at nominal beam energies of 1.06, 1.45 and 1.93 AGeV. The ^{58}Ni beam was accelerated by the *UNILAC/SIS* accelerator combination of the *GSI* /Darmstadt. The duty cycle was 75% with a spill length of 4 s. The average beam intensity corresponded to $5 \cdot 10^5$ particles per spill. The target consisted of a ^{58}Ni foil of $270\mu\text{m}$ thickness. This corresponds to an interaction probability of 0.5%. The average energy loss of the ^{58}Ni beam in this foil amounts to 0.005 AGeV and was neglected.

The particles produced by the Ni + Ni reactions were detected by the *FOPI* detector which is a modular detection system with almost 4π coverage. The *FOPI* detector is described in [12] [13]. Of particular importance for the present investigation are the central drift chamber *CDC* which is mounted inside the superconducting magnet with a solenoidal field of 0.6 T strength, and the forward plastic scintillation wall *PLA*. Both detector components have complete cylindrical symmetry, the *CDC* covers the polar angles from 32° to 150° in the laboratory frame and allows pions to be distinguished from baryons. The particle multiplicity measured by the *CDC* is labelled n_{CDC} , when pions are excluded

we use as quantity the measured baryonic charge $Z_{\text{CDC}}^{\text{bar}}$. The *PLA* covers the polar range from 7° to 30° , it allows the separation of particles only according to their charge number Z . The measured particle multiplicity in this case is labelled n_{PLA} . Similarly the total particle multiplicity is labelled n_{TOT} with $n_{\text{TOT}} = n_{\text{CDC}} + n_{\text{PLA}}$. Because of the inability of the *FOPI* detector at the time of the experiment to identify pions for polar angles smaller than 32° the solid angle of the pion identification amounts to around 8.2 sr. But pions emitted into the uncovered area of the complete solid angle can be reconstructed by employing the symmetry relation

$$f(\Theta, \Phi) = f(\pi - \Theta, \pi + \Phi), \quad (1)$$

where f may be any angle dependent observable and $\Theta, \Phi = \varphi$ refer to the *cm* frame. This relation is valid only for symmetric reactions. Including the remaining detection and geometrical thresholds it is estimated that after symmetrization around 90% of the pion momentum space becomes accessible.

In the present study we shall use the identical conventions which were used in ref.[1]. All quantities which refer to the laboratory(*lab*) or target frames will be labelled by small letters. The center of mass(*cm*) or fireball frames are generally characterized by capital letters. Exceptions are those quantities, like the transverse momentum, which remain unchanged under the transformation of frames. The magnitude of the transverse momentum p_t is given in units of $p_t^{(0)}$ where the index (0) indicates a normalization by the factor $(A \cdot P_{\text{proj}}/A_{\text{proj}})^{-1}$ and where A is the particle's mass number. Similarly the rapidity Y in the *cm* system is normalized by the factor $(Y_{\text{proj}})^{-1}$ and this quantity is labelled $Y^{(0)}$. In the present experiments the normalization factors for the pion transverse momentum have the values 9.47, 8.09, 7.02(GeV/c) $^{-1}$ for 1.06, 1.45, 1.93 AGeV bombarding energy, equivalently the normalization factors of the rapidities are 1.44, 1.26, 1.12.

The data from the drift chamber *CDC* were analyzed by using three different tracking algorithms as described in ref.[1]. The purpose of this threefold analysis is predominantly to obtain a measure of the systematic errors involved in the track finding and particle identification. Because of the smaller particle multiplicities, compared to the Au + Au reaction, the systematic errors are reduced in the present case. They are largest for the pion multiplicities where, for large impact parameters, they become as large as 10%. For other quantities, like the pion mean kinetic energies or the widths of their rapidity distributions, they always remain smaller than 5%. In [1] the uncertainty of measuring the pion transverse momenta from the curvature of the pion tracks was determined to increase from 4% to 7% in the range $0 < p_t < 1000$ MeV/c. From the accuracy of $\pm 2^\circ$ with which the forward *CDC* limit $\vartheta = 32^\circ$ is identified in the particle spectra one obtains a similar systematic uncertainty of 7% with which the pion *lab* momenta can be measured in forward direction. In this paper we generally quote only one error which is the larger one of the statistical and systematic errors. Normally the latter determines the error.

Table 1: Lower multiplicity boundaries $n_{\text{TOT}}(TM5)$, cross sections σ_{reac} , and deduced radii r_0 for the Au + Au (first row) and the Ni + Ni reactions

energy ($A\text{GeV}$)	$n_{\text{TOT}}(TM5)$ lower limit	σ_{reac} (barns)	r_0 (fm)
1.06	146	5.50 ± 0.50	1.14 ± 0.05
1.06	60	2.19 ± 0.24	1.08 ± 0.06
1.45	64	2.44 ± 0.29	1.14 ± 0.07
1.93	68	2.35 ± 0.21	1.12 ± 0.05

3 Experimental results

3.1 Charged particle multiplicities

The multiplicity distributions of charged particles measured with the forward scintillation detector *PLA* and the central drift chamber *CDC* vary only weakly for the three chosen bombarding energies. These spectra rise for small multiplicities n_{TOT} , their plateaus for large multiplicities are less well developed than in case of the heavier Au + Au reaction, c.f. Fig.6 of ref.[1]. It is common practice to subdivide the multiplicity distributions into 5 bins *TM1* to *TM5* where the upper bin *TM5* has its lower multiplicity boundary at half the plateau value, and where the other 4 bins have equal multiplicity widths. These bins select event classes of certain impact parameter ranges, with *TM1* corresponding to the most peripheral reactions, and *TM5* to the most central reactions. The values which define the lower multiplicity boundaries of the *TM5* bins are listed in table 1. The slight increase of this value with bombarding energy is mainly due to an increase of the charged pion multiplicity. The 'minimum bias' situation is defined by the condition that events are not selected according to their total charged particle multiplicity n_{TOT} .

After the integration of the multiplicity distributions over their total range, and after corrections because of acceptance losses for multiplicities $n_{\text{TOT}} \leq 8$, the total cross sections σ_{reac} for the 3 bombarding energies are deduced and listed in table 1. This table also includes the corresponding information from the Au + Au reaction. These cross sections define the nuclear radii r_0 via $r_0 = 0.5A^{-1/3} \sqrt{\sigma_{\text{reac}}/\pi}$ where A is the mass number of the target respectively projectile, and where it is assumed that both nuclei have sharp surfaces. The values of r_0 are listed in table 1. They are for all systems studied close to $r_0 = 1.12\text{fm}$ and therefore slightly smaller than the values deduced from electron scattering [14]. It was argued in ref.[1] that the agreement with electron scattering is improved when the smooth nuclear surface is taken into account.

It was already pointed out that the multiplicity n_{TOT} is related to the impact

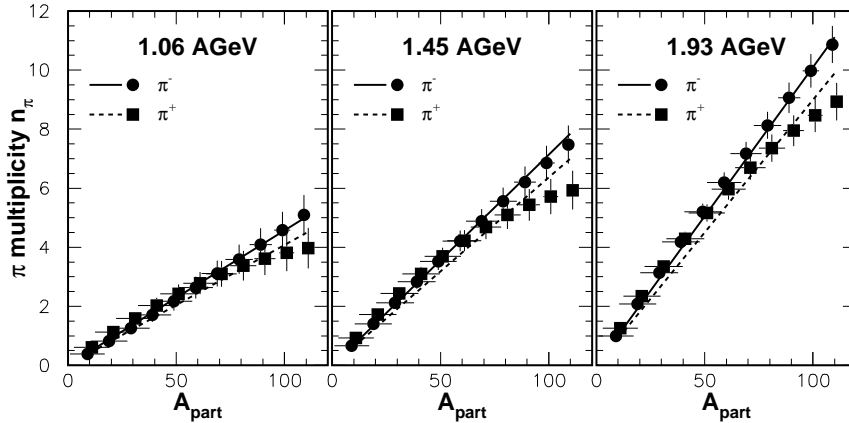


Figure 1: The dependence of the π^\pm multiplicities on the number of nucleons A_{part} in the fireball. The full and dotted lines present the extrapolations from the results of Harris et al.(see text)

parameter b and thus to the size of the nuclear fireball, expressed by the number A_{part} of participants. To deduce the quantitative relation between n_{TOT} and A_{part} requires to parametrize the nuclear density distribution by a Woods - Saxon form factor as was outlined in ref.[1]. Applying the identical procedures and also using the identical global quantities n_{TOT} , n_{PLA} , $Z_{\text{CDC}}^{\text{bar}}$, the number of charged pions n_{π^\pm} can be obtained as function of A_{part} . We show the dependence of n_{π^\pm} on A_{part} in Fig.1, where the measured pion multiplicities were used to calculate the mean multiplicities at regular intervals of A_{part} . The measured pion multiplicities were in all cases multiplied with a factor 1.1 to correct for the remaining detection inefficiencies [1]. This 10% correction of the pion multiplicities is predominantly caused by the $\vartheta = 32^\circ$ cut for pion transverse momenta $p_t < 0.6$, c.f. Fig.3. Its size was estimated using the *IQMD* model [15] or a thermal model in which pions are isotropically emitted with the measured mean kinetic energies. Owing to these models which both do not describe the experimental observations completely [1], the accuracy of this correction cannot be expected to be better than 50%. Within this limit the correction does not change with system mass or energy or impact parameter, since the pion momentum distributions do not change very much, as discussed later. The horizontal errors present the estimated accuracies with which A_{part} can be obtained from n_{TOT} , n_{PLA} , $Z_{\text{CDC}}^{\text{bar}}$, the vertical errors are predominantly systematic and present the uncertainties which were estimated by using different trackers. In addition the Fig.1 displays the expected pion multiplicities which one obtains by extrapolating the Fig.2 of [8] into the Ni + Ni system. The comparison with the expectation demonstrates that the dependence

Table 2: Expansion coefficients $a_i^{(2)}$ for the expansion of $n_\pi(A_{\text{part}})$ in powers of A_{part} for the Ni + Ni reactions

energy (AGeV)	π^-		π^+	
	$a_1^{(2)} \cdot 10^2$	$a_2^{(2)} \cdot 10^4$	$a_1^{(2)} \cdot 10^2$	$a_2^{(2)} \cdot 10^4$
1.06	4.22 ± 0.89	0.41 ± 0.71	5.76 ± 0.76	-1.96 ± 0.67
1.45	7.30 ± 1.26	-0.41 ± 0.94	8.73 ± 1.22	-3.02 ± 0.95
1.93	11.4 ± 1.53	-1.41 ± 1.18	12.5 ± 1.21	-4.12 ± 1.06

of n_{π^\pm} on A_{part} is not linear in A_{part} , but that the mean charged pion multiplicities should be close to the results obtained by Harris et al.[8] when extrapolated into the Ni + Ni system. In order to account for the measured non-linearities n_{π^\pm} was described by a power series of second order in A_{part} , i.e.

$$n_\pi(A_{\text{part}}) = a_1^{(2)} A_{\text{part}} + a_2^{(2)} A_{\text{part}}^2, \quad (2)$$

where the index $^{(2)}$ indicates the order of the expansion. The expansion coefficients $a_i^{(2)}$ are listed in table 2 for the three energies used. In a way described in ref.[1] the average number of pions per average number of participants can be deduced from the $a_i^{(2)}$ via

$$\frac{\langle n_\pi \rangle}{\langle A_{\text{part}} \rangle} = a_1^{(2)} + \frac{a_2^{(2)}}{2} A_0, \quad (3)$$

where A_0 is the total number of nucleons. The results are shown in table 3 which includes also the Au + Au reaction. Notice that these values depend on the order of the expansion. If only a 1. order expansion is chosen, as was additionally done in [1], the π^- multiplicities in the present case were not effected, but the π^+ multiplicities would be reduced by 15%. This would yield a similar increase of the π^- to π^+ ratios, but an 8% reduction of the total pion multiplicities. The total pion multiplicity $\langle n_\pi \rangle$ is calculated using the isobar models prediction [16]

$$n_{\pi^-} : n_{\pi^0} : n_{\pi^+} = (5N^2 + NZ) : (N^2 + 4NZ + Z^2) : (5Z^2 + NZ) \quad (4)$$

where in this case N, Z are the numbers of neutrons, respectively protons in the target or projectile. The eq.(4) holds if the pions are emitted by a resonance with isospin $I = 3/2$, and yields for the n_{π^-} to n_{π^+} ratio a value $R_\pi^{(t)} = 1.12$. This is in very good agreement with the experimental mean values of the ratio $R_\pi^{(e)} = \langle n_{\pi^-} \rangle / \langle n_{\pi^+} \rangle$ also shown in table 3, whereas in case of the Au +

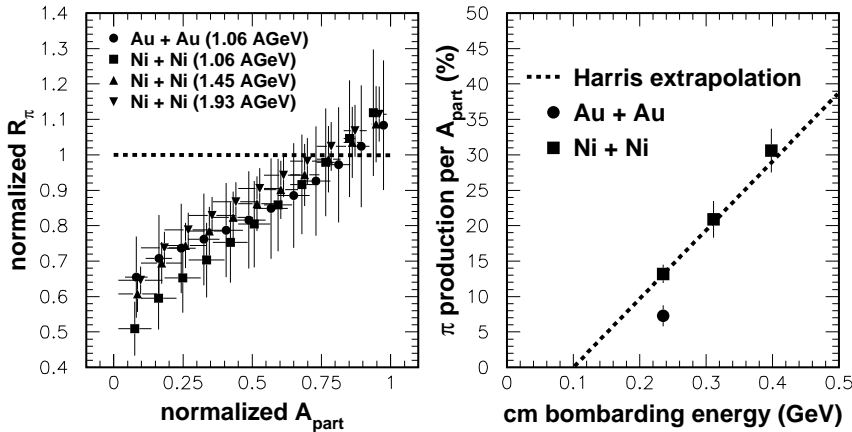


Figure 2: Left: The dependence of the normalized π^- to π^+ ratio $R_\pi^{(e)}/R_\pi^{(t)}$ on the scaled number of participants A_{part}/A_0 for different reactions and bombarding energies. The dotted line corresponds to $R_\pi^{(e)} = R_\pi^{(t)}$. Right: The comparison between the measured mean number of pions per participant and the extrapolation from the results of Harris et al.(see text)

Au reaction one finds a considerable disagreement between the model prediction $R_\pi^{(t)} = 1.95$ and the experimental value. If resonances with isospin $I = 1/2$ were also involved the ratios in eq.(4) would be replaced by

$$n_{\pi^-} : n_{\pi^0} : n_{\pi^+} = 2Z : (N + Z) : 2N \quad , \quad (5)$$

which is smaller than the experimentally observed value. One is, however, not allowed to conclude that this proves a contribution from $I = 1/2$ resonances in case of the Au + Au reaction, since eqs.(4,5) are valid only for first-generation decays and do not include multiple generations of resonances.

This result appears rather puzzling because the non-linear behavior of the pion multiplicities n_{π^\pm} nevertheless yields a functional dependence of the ratio $R_\pi^{(e)}$ on A_{part} which is very similar for all reactions studied. In order to demonstrate this similarity we have normalized $R_\pi^{(e)}$ to $R_\pi^{(t)}$ and A_{part} to A_0 , and these normalized quantities are plotted in Fig.2. After the normalization the π^- to π^+ ratio increases almost linearly with the normalized A_{part} , for small values of A_{part} , i.e. large impact parameters, one finds an apparent deficit of π^- whereas for central collisions there appears to be a deficit of π^+ . Notice that the dependence of $R_\pi^{(e)}$ on A_{part} does not disappear when A_{part} is determined by means of the charged particle multiplicity but employing a different method, since a different method will not change the values of $R_\pi^{(e)}$ although it might change their exact dependence on A_{part} . Nevertheless, the condition of total charge conservation

Table 3: Average number of pions n_π per average number of participants A_{part} and average n_{π^-} to n_{π^+} ratio for Au + Au (first row) and Ni + Ni reactions. Only systematic errors are shown, the statistical errors are in the order of 10% of the systematic errors

energy(AGeV)	$\frac{\langle n_{\pi^-} \rangle}{\langle A_{\text{part}} \rangle} (\%)$	$\frac{\langle n_{\pi^+} \rangle}{\langle A_{\text{part}} \rangle} (\%)$	$\frac{\langle n_\pi \rangle}{\langle A_{\text{part}} \rangle} (\%)$	$R_\pi^{(e)}$
1.06	3.08 ± 0.37	1.82 ± 0.43	7.26 ± 0.84	1.69 ± 0.26
1.06	4.46 ± 0.51	4.62 ± 0.41	13.62 ± 1.39	1.19 ± 0.07
1.45	7.06 ± 0.80	6.98 ± 0.75	21.05 ± 3.29	1.04 ± 0.17
1.93	10.55 ± 1.01	10.07 ± 0.79	30.92 ± 3.83	1.05 ± 0.13

can induce a correlation between the measured particle multiplicity and the ratio $R_\pi^{(e)}$ which will be discussed in more detail in section 4.

In Fig.2 we have also plotted the dependence of the average number of all pions per participant on the bombarding energy. As expected the Ni + Ni system closely follows the systematics obtained by Harris et al.[8], whereas the pions from the Au + Au system are reduced in number by almost a factor 2. It was pointed out in ref.[1] that this reduction is confirmed in measurements of the π^\pm production by the *KaoS* collaboration [11], and in case of the π^0 by the *TAPS* collaboration [11]. Both collaborations use detectors which have a solid angle smaller than 4π and therefore require the extrapolation from the measured range into complete solid angle. This extrapolation is not simple since the angular distributions of pions are non-isotropic, c.f. section 3.2, and since the anisotropy depends on system mass. But the observed reduction is of a size that even a better extrapolation procedure will not reconcile these results from different experiments with the expectations one obtains by extrapolating from the light-mass to heavy-mass systems.

3.2 Phase space distributions of charged pions

In the previous investigation of the Au + Au reaction the phase space distributions of π^\pm were found to be non-thermal, requiring at least two temperatures and a non-isotropic angular distribution for their parametrizations. Similar observations are made in the present case of the Ni + Ni reaction as will be shown in detail in the following subsections.

The Fig.3 shows a total view onto the π^- and π^+ momentum space distributions under minimum bias condition in case of the Ni + Ni reaction at 1.06 AGeV bombarding energy. Also shown are the curves of constant momentum $P = 0.2, 0.4, 0.6$ GeV/c to illustrate the deviations from a pure thermal behavior, and as broken curve the $\vartheta = 32^\circ$ geometrical limit of the *CDC*. Pions at smaller angles were not measured but obtained by employing the reflection symmetry

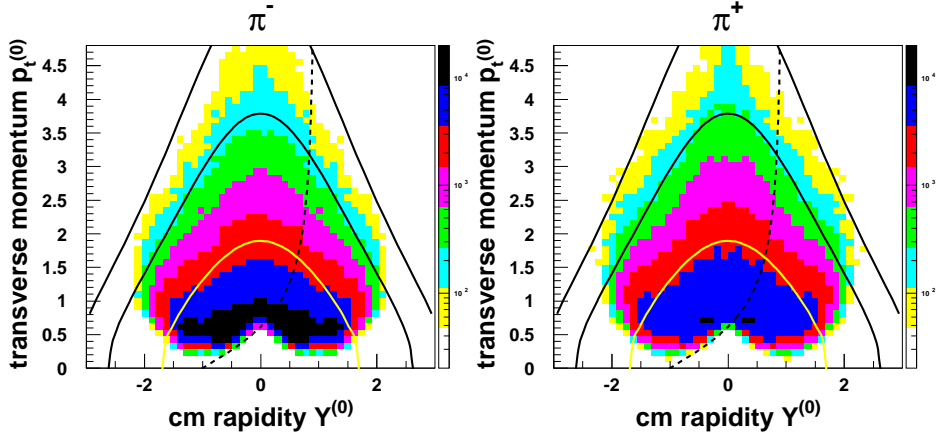


Figure 3: The momentum space distribution under minimum bias condition for π^- and π^+ at 1.06 AGeV bombarding energy. The full curves are displayed for pion momenta $P = 0.2, 0.4, 0.6$ GeV/c, the dotted curves display the $\vartheta = 32^\circ$ forward boundary of the CDC. The invariant cross section $d^2\sigma/(p_t dp_t dY^{(0)})$ is displayed in arbitrary units on a logarithmic scale

around $Y^{(0)} = 0$. The Fig.3 should be compared to the equivalent Fig.10 in ref.[1] to see that differences between the pion emission from the Ni + Ni and Au + Au are only small. Nevertheless such differences exist, and their detailed exposure is the subject of the following subsections.

3.2.1 Kinetic energies

The kinetic energy distributions of π^- and π^+ from the Ni + Ni reactions have, at all bombarding energies studied, concave shape, and therefore two Boltzmann distributions with different temperatures, a low temperature $T_{l,\pi}$ and a high temperature $T_{h,\pi}$, are needed to fit these distributions in the frame of a thermal picture. This is similar to the Au + Au reaction presented in ref.[1], where the Fig.12 showed a representative example of the measured distributions at $\Theta = 130^\circ$. Similar to the Au + Au reaction is also that the extracted values for $T_{h,\pi}$ appear to increase for emission angles $\Theta \geq 140^\circ$. The angular dependence of the low and high-temperature values is plotted in Fig.4. The values show considerable fluctuations, the fluctuations are inherent to our procedure which fits a sum of two exponentials to a distribution which only slightly deviates from a pure exponential behavior. The temperature increase at backward angles is seen most strongly for the π^+ , in order to illustrate the size of the increase the Fig.5 compares the π^- spectrum at $\Theta = 90^\circ$ to the π^+ spectrum at $\Theta = 150^\circ$, where the pions were measured at 1.06 AGeV bombarding energy. The Fig.4 also reveals that T_{l,π^+} is systematically larger than T_{l,π^-} , whereas for $\Theta < 140^\circ$ the

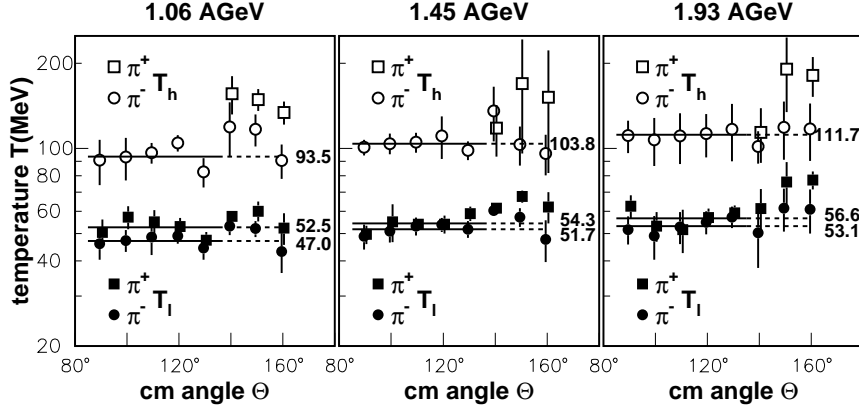


Figure 4: The apparent pion temperatures $T_{1,\pi}$ and $T_{h,\pi}$ for different cm angles Θ . The lines display the the mean values in the range $85^\circ < \Theta < 135^\circ$

Table 4: Apparent pion temperatures $T_{1,\pi}$ and $T_{h,\pi}$ and mean ratio of the low-temperature to high-temperature component R_T for Au + Au (first row) and Ni + Ni reactions. The error shown is the larger of the statistical and systematic errors for a given entry

energy(AGeV)	T_{1,π^-} (MeV)	T_{1,π^+} (MeV)	$T_{h,\pi}$ (MeV)	R_T
1.06	42.2 ± 2.7	49.4 ± 3.7	96.4 ± 5.1	0.75 ± 0.36
1.06	47.0 ± 1.9	52.5 ± 3.6	93.5 ± 8.0	1.30 ± 0.81
1.45	51.7 ± 1.9	54.3 ± 3.3	103.8 ± 4.9	1.15 ± 0.37
1.93	53.1 ± 5.7	56.6 ± 4.4	111.7 ± 9.5	1.06 ± 0.80

fits to the energy distributions are consistent with the assumption that T_{h,π^+} is equal to T_{h,π^-} . The temperature values obtained from such fits depend on the fit range. In our analysis the π^- kinetic energy spectra were fitted in the range from 50 to 750 MeV, whereas the fit range for the π^+ kinetic energy spectra varies with angle Θ : for $\Theta = 90^\circ$ the range is from 50 to 375 MeV, the upper limit has increased to 750 MeV for $\Theta = 130^\circ$. As pointed out in ref.[1] this angular variation of the fit range is necessary to separate π^+ from protons in the analysis.

In accordance with the analysis of the pion energy spectra performed in ref.[1], and because of the increase of the angular cross section $d\sigma/d\Omega$ for $\Theta \geq 140^\circ$ (see below), we have extracted the average pion temperatures only from pions emitted into the angular range $40^\circ < \Theta < 140^\circ$, the values are listed in table 4 and shown in Fig.4. The values of $T_{h,\pi}$ agree with an independent analysis of the present

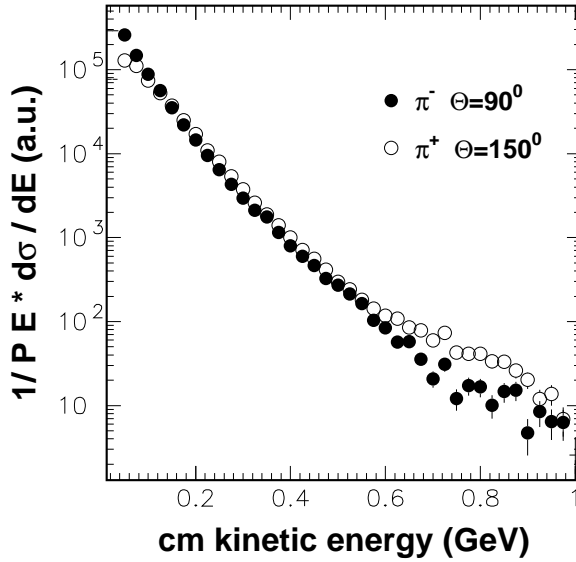


Figure 5: The kinetic energy spectra of π^- and π^+ observed at 1.06 AGeV bombarding energy at different cm angles Θ

data based on the transverse momentum spectra [17], but they are significantly larger (≈ 20) MeV than those obtained by the *KaoS* collaboration [10]. In the latter case the π^+ momentum spectra, measured at $\vartheta = 44^\circ \pm 4^\circ$ in the *lab* frame, were analyzed. Whether this difference in the method or different fit ranges are responsible for the discrepancy is not clear. The table 4 also contains the ratio R_T , which is the ratio between the low-temperature component $I_{l,\pi}$ and the high-temperature component $I_{h,\pi}$, and it contains the equivalent results from the Au + Au reaction. The intensities $I_{l,\pi}$ and $I_{h,\pi}$ were calculated by integration over the Boltzmann distributions with temperature $T_{l,\pi}$, respectively $T_{h,\pi}$. The differences between T_{l,π^+} and T_{l,π^-} , which amount in the average to 3.9 ± 1.5 MeV in case of Ni + Ni, but to twice this value in case of Au + Au, has its origin in the Coulomb repulsion, respectively attraction between the pions and the positively charged baryonic matter. Therefore the ratio R_T is influenced by the Coulomb interaction, and to compensate this effect the values of R_T quoted in table 4 are the mean values between π^- and π^+ . Notice that the large errors assigned to the values of R_T are mainly systematic and due to the fact that R_T changes more with angle for $\Theta < 140^\circ$ than the temperatures.

Both pion temperatures, the low $T_{l,\pi}$ temperature and the high $T_{h,\pi}$ temperature, increase slightly with beam energy. Similarly also the relative contribution of pions with high temperatures increases, but this component never exceeds the contribution of low-temperature pions in the cases of the Ni + Ni reactions. This is different in the Au + Au reaction where already at 1.06 MeV bombarding energy the high-temperature component is stronger than the low-temperature

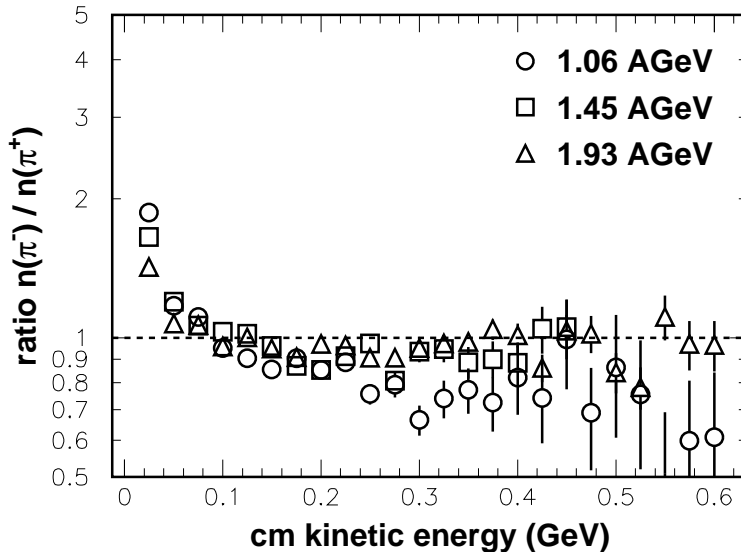


Figure 6: The mean n_{π^-} to n_{π^+} ratio in the range $85^\circ < \Theta < 135^\circ$ as function of the cm kinetic energy. The dotted line corresponds to equal numbers of π^- and π^+

component.

The use of the term 'temperature' in discussing the kinetic energy distributions of charged pions should not be confused with the true thermodynamic temperature describing unordered motion. Even in the case that pions thermalize in nuclear matter their finite mean free path adds a zero point energy to their thermal energies because of their small mass. The size of this quantum effect is in the order of 25 MeV, its general dependence on mass and localization of the pions was calculated in ref.[18]. In our present analysis the temperature is solely used as a fit parameter to reproduce the concave shapes of the energy distributions. Its small sensitivity to the bombarding energy indicates, that the freeze-out conditions of pions do not depend strongly on the initial conditions, on the other hand they are not completely independent of these conditions. It is obvious that to make the differences visible, the experimental accuracies have to be accordingly high, and the fit conditions have to be defined in a consistent way.

For the sake of completeness and in accordance with the deduced pion temperatures we display in Fig.6 the ratio of the kinetic energy spectra of π^- to π^+ under minimum bias conditions, where only the cm angles $90^\circ < \Theta < 135^\circ$ are included. For the three bombarding energies studied the dependence of this ratio on the pion kinetic energy changes only very little and is, except for the smaller values at small kinetic energies, similar to the Au + Au case, c.f. Fig.13 in ref.[1]. Notice in particular that the intersection with one occurs in all systems at kinetic

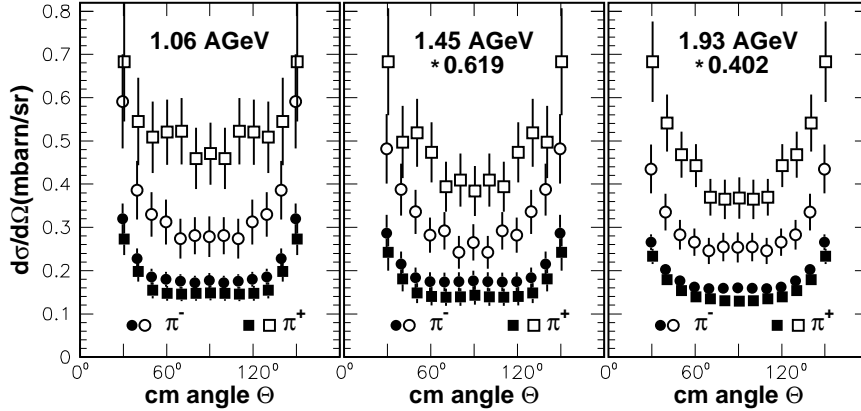


Figure 7: The pion angular distributions for peripheral (open symbols) and central (full symbols) reactions

energies less than 300 MeV. The global dominance of the π^- over the π^+ , expressed by $R_\pi^{(e)} > 1$ is therefore caused by the more abundant low-energy pions, at larger energies this relation appears to be reversed. The observation that the π^- yield becomes smaller than the π^+ yield for kinetic energies above 100 MeV is linked to the reactions with large impact parameter, c.f. Fig.1 and Fig.2. In the case of central ($TM5$) collisions the π^- to π^+ ratio approaches the value one for kinetic energies above 200 MeV. Accordingly the shape of the kinetic energy spectra of pions, i.e. the apparent pion temperatures, do not change significantly with impact parameter, but the yields do.

3.2.2 Angular distributions

The angular distributions of charged pions were found in previous experiments to be non-isotropic with a pronounced enhancement at forward and backward angles [16]. This feature is similarly observed in the present Ni + Ni reactions at all energies, c.f. Fig.7. In the Fig.7 the measured angular distributions $d\sigma/d\Omega$ are displayed under the selection criteria of peripheral ($TM1$) and central ($TM5$) collisions. All measured pions with kinetic energies above 50 MeV are included. Notice that the reversal in the sizes of the π^- and π^+ cross sections between $TM1$ and $TM5$ is a phenomenon similarly seen in Fig.1 or Fig.2. Since in the elementary $N + N \rightarrow N + N + \pi$ reaction pions are also preferentially emitted into forward and backward angles, one possible explanation for the anisotropy found in nucleus - nucleus reactions is based on first-chance collisions in the dilute surfaces of the colliding nuclei. Alternatively the rescattering of pions in spectator matter yields a similar angular anisotropy. It was argued in ref.[1]

that this latter mechanism could also explain the increase of the apparent pion temperatures at forward and backward angles. Contributions from spectators are always assumed to be present in the phase space distributions of baryons, and a similar anisotropy in the angular distributions of protons under minimum bias conditions is readily interpreted as due to spectator decay. Indeed, the forward/backward enhancement changes more strongly with impact parameter in the Au + Au reaction than in the Ni + Ni reactions, and this change is different for π^- than for π^+ . In the first reaction the anisotropy $\sigma(150^\circ)/\sigma(90^\circ)$ increases between *TM5* and *TM1* by a factor 1.9 ± 0.2 for π^- and 1.4 ± 0.2 for π^+ , whereas in the second reactions the corresponding factors are 1.3 ± 0.2 and 1.0 ± 0.2 independent of the bombarding energy. The differences in the surface to volume ratios for Au and Ni, and the effects of the Coulomb attraction, respectively repulsion may be responsible for this behaviour of the pion angular distributions. It suggests that even in central collisions a large part of the nucleons is not stopped in Ni + Ni reactions.

The pion angular distributions reveal another peculiarity at angles around the transverse direction $\Theta = 90^\circ$. Whereas pions from central collisions of the Au + Au system display a clearly discernible enhancement of the emission into this angular range, c.f. Fig.17 of ref.[1], this enhancement is not observed for pions from the central Ni + Ni collisions at all energies studied. Earlier measurements of the pion angular distributions from light-mass systems gave a similar result [16], i.e. a flat $d\sigma/d\Omega$ at angles around $\Theta = 90^\circ$. Indeed, the transverse pion enhancement in the Au + Au central collisions constitutes the most direct evidence that the pion phase space distributions change with system mass at bombarding energies around 1 AGeV. The cause for this change is not understood. It is reminiscent of the predicted hydrodynamical flow in heavy systems when the nuclear compression approaches values of three times normal nuclear density [19]. But it is not clear why this is observed in the pion channel when it is most likely not present in the baryon channels [20]. With this respect it should be remembered that apparent pion flow phenomena are quite often interpreted as caused by pion absorption in the nuclear environment [21][22].

3.2.3 Rapidities

The forward/backward anisotropy seen in the pion angular and temperature distributions also determines the shape of the pion rapidity distributions. These are displayed in Fig.8, they are obtained from the complete phase space distributions shown in Fig.3 for a special case, by a projection onto the rapidity axis with p_t thresholds of $p_t > 85$ MeV/c (1.06), 100 MeV/c (1.45), 115 MeV/c (1.93), where the number in brackets specifies the bombarding energy in units of AGeV for which these p_t cuts were applied. The dotted curves in Fig.8 show the expected rapidity spectra, if pions were isotropically emitted with the two temperatures $T_{l,\pi}$ and $T_{h,\pi}$ determined in subsection 3.2.1. It is obvious that the

Table 5: Parameters of the three-source fits to the pion rapidity spectra under minimum bias condition for the Au + Au (first row) and Ni + Ni reactions. Notice that the values for the widths σ are presented in units of $Y^{(0)}$. The numbers in parenthesis give the systematic error in the last 2 digits. The statistical error is of the order (05) for $R_{Y,\pi}$ and (02) for $\sigma_{0,\pi}$, $\sigma_{1,\pi}$

energy(AGeV)	R_{Y,π^-}	σ_{0,π^-}	σ_{1,π^-}	R_{Y,π^+}	σ_{0,π^+}	σ_{1,π^+}
1.06	1.68(21)	0.45(04)	0.40(03)	1.52(14)	0.45(03)	0.42(03)
1.06	1.21(05)	0.48(01)	0.45(01)	1.16(07)	0.46(01)	0.47(02)
1.45	1.54(15)	0.49(01)	0.42(02)	1.30(10)	0.48(01)	0.44(02)
1.93	2.68(13)	0.51(01)	0.38(03)	2.43(34)	0.53(02)	0.39(03)

rapidity distributions deviate from these expectations, the deviations become less visible with increasing energy. In ref.[1] it was assumed that the excess intensity at rapidities around $|Y^{(0)}| = 1$ is due to rescattering by spectator matter, and the strength of this process was estimated by fitting the measured spectra with three Gaussian distributions located at $Y^{(0)} = -1, 0, +1$, where the Gaussians at $Y^{(0)} = \pm 1$ have to be identical for a symmetric reaction. This procedure was repeated in case of the Ni + Ni reaction. As in the Au + Au case the fit parameters, i.e. the width $\sigma_{Y,\pi}$ of the Gaussians in units of $Y^{(0)}$, and their relative intensities $R_{Y,\pi} = I_{0,\pi}/(I_{1,\pi} + I_{-1,\pi})$ do not change by more than 20% with impact parameter. Therefore the table 5 presents the values of $\sigma_{Y,\pi}$ and $R_{Y,\pi}$ only under minimum bias condition, in Fig.9 the ratio $R_{Y,\pi}$ is plotted for the different impact parameters and for the three bombarding energies of the Ni + Ni reaction. In addition we show in Fig.9 the widths $\sigma_{Y,\pi}$ as functions of bombarding energy this time in units of the unnormalized rapidity Y . The ratio $R_{Y,\pi}$ and the width $\sigma_{0,\pi}$ increase with bombarding energy, the widths $\sigma_{1,\pi}, \sigma_{-1,\pi}$ stay constant within their errors. This indicates that the number of pions being rescattered decreases with energy, and that the separation into 3 pion sources becomes increasingly ambiguous. At energies above 2 AGeV the rescattered pions from the spectator sources are almost completely masked by the non-rescattered pions from the central source. Note, however, that the pion angular distributions still show clear evidence for the presence of the rescattering mechanism at even the highest bombarding energy. Compared to the Au + Au reaction at 1.06 AGeV the Ni + Ni reaction at the same energy has a stronger rescattering signal, and this rescattering contribution to the pion rapidity spectra varies less with impact parameter than observed in the former reaction. These observations are the prominent indicators from the pions momentum space distributions that the nuclear corona phenomena and the related formation of nuclear spectators are different in the Ni + Ni and Au + Au systems. And it might provide the basis on which one might eventually find the cause for the transverse pion enhancement

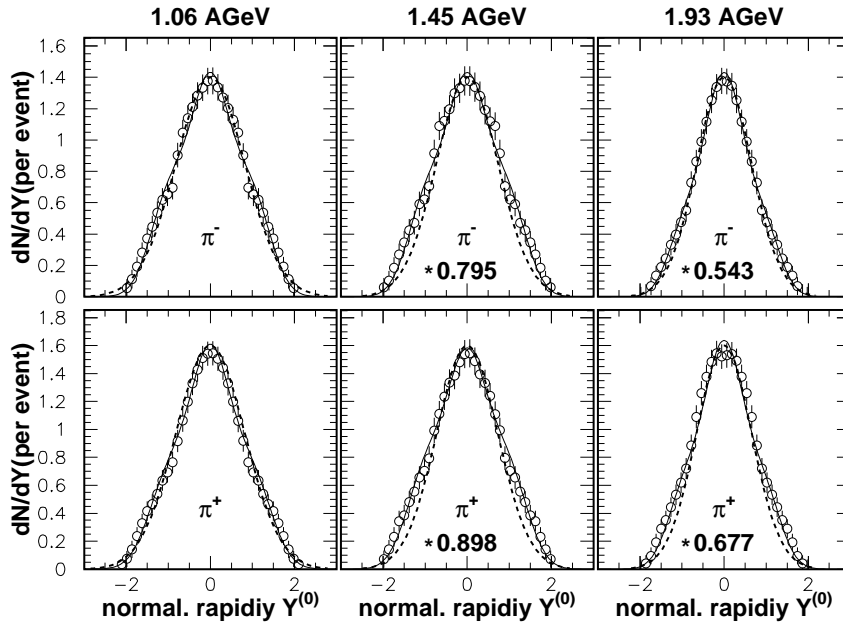


Figure 8: The pion rapidity spectra at different bombarding energies. The full curves show the fit by 3 Gaussian distributions (see text), the dotted curves are the thermal expectations assuming two temperatures $T_{l,\pi}$ and $T_{h,\pi}$

in central Au + Au collisions.

4 Summary and discussion

The results of this investigation should be discussed in relation to the study of pion production in the Au + Au system which contains almost four times as many nucleons. The total number of pions produced at a given energy is therefore larger in the heavier system, but when normalized to the number of participants the Ni + Ni system produces almost two times more pions at 1.06 AGeV than the Au + Au system. Furthermore the Ni result is in agreement with equivalent results from the Ar + KCl and the La + La systems studied by Harris et al.[8]. The surface to volume ratio varies from the Ni to the La system (1.34) more than from the La to Au system (1.12), and thus it is difficult to attribute the reduction of the π^\pm yield in the Au + Au case to an enhanced pion absorption in the larger fireball volume. To decide whether or not absorption is responsible for the reduced π^\pm yields, the independence of the normalized number of pions for system masses below $A_0 = 280$ should be confirmed, e.g. for the $A_0 = 200$ system. Considering the fact that the pion angular distributions depend on the system mass, it is not sufficient to do this test at midrapidity but it should be conducted over the complete solid angle.

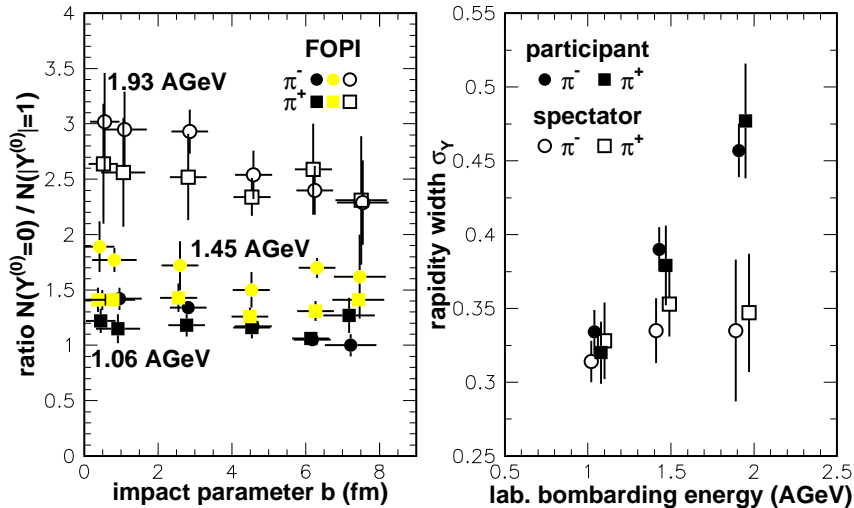


Figure 9: Left: The impact parameter dependence of the intensity ratios R_Y between pions from the fireball and pions from the spectators. Right: The energy dependence of the widths σ_Y of the pion rapidity distributions from the fireball and the spectators under minimum bias conditions

The alternative explanation for the reduced production of pions in the Au + Au system might be an enhanced flow of energy into collective motion which was recently observed in central collisions, although at lower energies [20]. This will decrease the energy available to excite baryon resonances. At energies around 1 AGeV pions are considered to mainly originate from the decay of heavy baryon resonances, where the $\Delta(1232)$ resonance dominates the pion production. Nevertheless, theoretical studies have shown that resonances up to a mass of 1.9 GeV/ c^2 have to be included to explain the pion spectra measured in Au + Au reactions [23]. The excitation of such resonances is seen in the concave shape of the π kinetic energy spectra. The apparent higher temperature $T_{h,\pi}$ is a signal for the presence of resonances above the lowest lying $\Delta(1232)$ resonance, as will be discussed in more detail in a forthcoming paper [24]. With this respect it is interesting to notice that $T_{h,\pi}$ is larger in the Au + Au reaction than in the Ni + Ni reaction at the same energy, and that also the contribution of the high-temperature component is larger in the Au than in all the Ni cases studied. This is a puzzling result, since an enhanced excitation of the higher baryon resonances should lead to an increase in the number of pions, because the 2π decay channel becomes more important. The conflict can be resolved in a simple way, if baryon resonances are only excited via $N + N$ collisions in the early compression phase of the collision. In the later expansion phase their decay by pion emission will

produce second and subsequent generations of resonances, not only in the fireball but also in the cold spectator matter. It is reasonable to assume that the number of resonance generations is larger in the heavier system, and that the competing $N + B \rightarrow N + N$ channel causes a loss of pions. In this case the total pion reduction would be proportional to a power law with the number of generations in the exponent.

Coulomb effects are present in the pion spectra, most indicative is the difference between the values of the low temperature T_{1,π^-} and T_{1,π^+} . This difference is only half as large in the Ni + Ni reaction than in the Au + Au reaction, and appears to be independent of bombarding energy. On the other hand the π^- to π^+ ratio also depends on the size of the fireball, expressed by the number of participants A_{part} . And this dependence, when properly normalized, is found to be independent of the system mass or energy. It has a universal dependence with too few π^- at peripheral reactions, and too few π^+ at central reactions. The latter might be due to the condition that the total charge is conserved. This condition and the requirement that for minimum impact parameter the measured particle multiplicity attains its maximum value selects events with large numbers of π^- , i.e. with large $R_{\pi}^{(e)}$ values. It is easy to see that the two conditions

$$\begin{aligned} Z^{\text{bar}} + (1 + R_{\pi}^{(e)})n_{\pi^+} &= \text{max} \\ Z^{\text{bar}} + (1 - R_{\pi}^{(e)})n_{\pi^+} &= \text{const} \end{aligned}$$

are the better fulfilled the larger $R_{\pi}^{(e)}$. Of course, $R_{\pi}^{(e)}$ in these equations cannot grow unlimited, it is bound by isospin and baryon conservation. But it is conceivable that it becomes largest when the number of measured particles is largest. In the case of peripheral reactions the pion rescattering process in spectator matter is probably non negligible in determining the π^- to π^+ ratio. The impact parameter dependence of the pion angular distributions is suggestive: In both systems, i.e. Au + Au and Ni + Ni, the forward/backward enhancement in peripheral reactions is stronger for π^- than for π^+ . Interpreted as due to rescattering, the rescattering process in spectator matter would then be stronger for π^- than π^+ , and the Coulomb attraction between the π^- and the positively charged spectators offers a possible explanation for this preference. The preferred absorption of π^- in spectator matter, without reemission because of the $N + B \rightarrow N + N$ channel, would also mean that pion absorption is an important process to heat the spectators. In addition the preferred absorption of negative pions should cause the decay products of the spectator to become more neutron-rich. The effects the Coulomb potential has on the ratio $R_{\pi}^{(e)}$ was recently studied in a theoretical paper by Teis et al. [25]. Whereas its dependence on the pion kinetic energies, c.f. Fig.6, is quite well reproduced, the dependence on the number of participants A_{part} deduced from the measured particle multiplicities is not studied in similar detail.

With respect to the pion 'temperatures' $T_{1,\pi}$ and $T_{h,\pi}$ listed in table 4, we want to reiterate that these should be only considered as fit parameters to the

concave shapes of the kinetic energy spectra. Their values depend on the chosen fit range. If the fit range is increased it is very probable that, to obtain a good fit, also the multitude of temperatures has to be increased. This is the reason why the upper energy boundary in case of the π^- spectra was limited to 750 MeV. The other reason is that the exact shape of the kinetic energy spectra at large kinetic energies, when the cross section has dropped by several orders of magnitude, depends on an accurate estimate of the background and on the way pions are selected from the data. The identification of pions with large energies, i.e. large momenta, requires to determine these momenta with high precision by the tracking algorithm. Above 750 MeV the standard deviation of the *lab* momentum in forward direction becomes larger than 7% [1] and this is considered inadequate to identify such rare pions with the required precision. Nevertheless, the systematic variations of $T_{l,\pi}$ and $T_{h,\pi}$ with system mass and energy allows one to make important conclusions. If the observed pions are assumed to be exclusively remnants from the decay of baryon resonances, then the increase of $T_{l,\pi}$ and $T_{h,\pi}$ with increasing energy and mass is related to the change of the number of resonances involved and on their excitation profile at pion freeze-out times. In principle the pion energy spectra can be used to derive information about these quantities. This line of analysis shall be followed in a forthcoming paper [24]. On the other hand if the high-temperature component is interpreted as due to pions thermalized in the nuclear medium [26], the values of $T_{h,\pi}$ allow one to deduce the fireball temperatures at pion freeze-out times. This line of analysis is followed in ref.[17]. However, one should not forget the problems which are caused by the quantum nature of pions and which were mentioned in subsection 3.2.1.

Acknowledgement This work was supported in part by the Bundesministerium für Forschung und Technologie under contract 06 HD 525 I(3) and by the Gesellschaft für Schwerionenforschung under contract HD Pel K.

References

- [1] **FOPI** collaboration: D. Pelte et al., Z. Phys. A **357**, 215(1997)
- [2] P. Braun-Munzinger, J. Stachel, J.P. Wessels, N. Xu, Phys. Lett. **B344**, 43(1995)
- [3] Bao-An Li, W. Bauer, Phys. Rev. C **44**, 450(1991)
- [4] P. Danielewicz, Phys. Rev. C **51**, 716(1995)
- [5] S. Nagamiya, M.-C. Lemaire, E. Moeller, S. Schnetzer, G. Shapiro, H. Steiner, I. Tanihata, Phys. Rev. C **24**, 971(1981)
- [6] S. Nagamiya, Phy. Rev. Lett. **49**, 1383(1982)

- [7] R. Brockmann, J.W. Harris, A. Sandoval, R. Stock, H. Stroebele, G. Odyniec, H.G. Pugh, L.S. Schroeder, R.E. Renfordt, D. Schall, D. Bangert, W. Rauch, K.L. Wolf, Phys. Rev. Lett. **53**, 2012(1984)
- [8] J.W. Harris, G. Odyniec, H.G. Pugh, L.S. Schroeder, M.L. Tincknell, W. Rauch, R. Stock, R. Bock, R. Brockmann, A. Sandoval, H. Ströbele, R.E. Renfordt, D. Schall, D. Bangert, J.P. Sullivan, K.L. Wolf, A. Dacal, C. Guerra, M.E. Ortiz, Phys. Rev. Lett. **58**, 463(1987)
- [9] **TAPS** collaboration: O. Schwalb et al., *GSI* report GSI-93-38(1993), and Phys. Lett. **B321**, 20(1994)
- [10] **KaoS** collaboration: C. Müntz et al., *GSI* report GSI-93-41(1993), Z. Phys. A **352**, 175(1995), Z. Phys. A **357**, in print
- [11] P. Senger, in: Multiparticle Correlations and Nuclear Reactions, ed. by J. Aichelin and D. Ardouin (World Scientific Publ. Co., 1994), page 285
- [12] **FOPI** collaboration: A. Gobbi et al., Nucl. Instr. Meth. A **324**, 156(1993)
- [13] **FOPI** collaboration: J.L. Ritman et al., Nucl. Phys. B - Proc. Suppl. **44**, 708(1995)
- [14] R. Hofstadter, Rev. Mod. Phys. **28**, 214(1956)
- [15] J. Aichelin, Phys. Rep. **202**, 233(1991)
- [16] R. Stock, Phys. Rep. **135**, 259(1986)
- [17] **FOPI** collaboration: B. S. Hong et al., to be published
- [18] H. Merlitz, D. Pelte, Z. Phys. A **357**, 175(1997)
- [19] H. Stöcker, W. Greiner, Phys. Rep. **137**, 277(1986)
- [20] **FOPI** collaboration: W. Reisdorf et al., Nucl. Phys. **A612**, 493(1997)
- [21] S.A. Bass, C. Hartnack, H. Stöcker, W. Greiner, Phys. Rev. C **51**, 3343(1995)
- [22] Bao-An Li, Phys. Lett. B **319**, 412(1993)
- [23] S. Teis, W. Cassing, M. Effenberger, A. Hombach, U. Mosel, G. Wolf, Z. Phys. A. **356**, 421(1997)
- [24] **FOPI** collaboration: M. Eskef et al., to be published
- [25] S. Teis, W. Cassing, M. Effenberg, A. Hombach, U. Mosel, G. Wolf, nucl-th/9701057
- [26] **E814** collaboration: J. Barrette et al., Phys. Lett. B **351**, 93(1995)